

REPORT DOCUMENTATION PAGE

Form Approved OMB NO. 0704-0188

The public reporting burden for this collection of information is estimated to average 1 hour per response, including the time for reviewing instructions, searching existing data sources, gathering and maintaining the data needed, and completing and reviewing the collection of information. Send comments regarding this burden estimate or any other aspect of this collection of information, including suggestions for reducing this burden, to Washington Headquarters Services, Directorate for Information Operations and Reports, 1215 Jefferson Davis Highway, Suite 1204, Arlington VA, 22202-4302. Respondents should be aware that notwithstanding any other provision of law, no person shall be subject to any penalty for failing to comply with a collection of information if it does not display a currently valid OMB control number.

PLEASE DO NOT RETURN YOUR FORM TO THE ABOVE ADDRESS.

1. REPORT DATE (DD-MM-YYYY) 14-06-2016	2. REPORT TYPE Final Report	3. DATES COVERED (From - To) 15-Mar-2013 - 14-Mar-2016		
4. TITLE AND SUBTITLE Final Report: Optical Spectroscopy and Imaging of Correlated Spin-Orbit Phases		5a. CONTRACT NUMBER W911NF-13-1-0059		
		5b. GRANT NUMBER		
		5c. PROGRAM ELEMENT NUMBER 611102		
6. AUTHORS David Hsieh		5d. PROJECT NUMBER		
		5e. TASK NUMBER		
		5f. WORK UNIT NUMBER		
7. PERFORMING ORGANIZATION NAMES AND ADDRESSES California Institute of Technology Office of Sponsored Research 1200 E. California Blvd. Pasadena, CA 91125 -0001		8. PERFORMING ORGANIZATION REPORT NUMBER		
9. SPONSORING/MONITORING AGENCY NAME(S) AND ADDRESS (ES) U.S. Army Research Office P.O. Box 12211 Research Triangle Park, NC 27709-2211		10. SPONSOR/MONITOR'S ACRONYM(S) ARO		
		11. SPONSOR/MONITOR'S REPORT NUMBER(S) 63606-PH.12		
12. DISTRIBUTION AVAILABILITY STATEMENT Approved for Public Release; Distribution Unlimited				
13. SUPPLEMENTARY NOTES The views, opinions and/or findings contained in this report are those of the author(s) and should not be construed as an official Department of the Army position, policy or decision, unless so designated by other documentation.				
14. ABSTRACT Over the course of this ARO award we constructed three ultrafast laser based probes (nonlinear optical rotational anisotropy, nonlinear optical microscopy and time-resolved optical reflectivity) to search for novel electronic phases in correlated electron materials. Using these techniques, we completed five major scientific projects. 1) We discovered previously unresolved oxygen sub-lattice distortions in layered perovskite iridates, which explain the anomalous magneto-elastic coupling and basal plane ferromagnetism observed in Sr ₂ IrO ₄ and Sr ₃ Ir ₂ O ₇				
15. SUBJECT TERMS Ultrafast optical spectroscopy, nonlinear optical spectroscopy, iridates, cuprates				
16. SECURITY CLASSIFICATION OF: a. REPORT UU		17. LIMITATION OF ABSTRACT UU	15. NUMBER OF PAGES	19a. NAME OF RESPONSIBLE PERSON David Hsieh
b. ABSTRACT UU				19b. TELEPHONE NUMBER 626-395-4758
c. THIS PAGE UU				

Report Title

Final Report: Optical Spectroscopy and Imaging of Correlated Spin-Orbit Phases

ABSTRACT

Over the course of this ARO award we constructed three ultrafast laser based probes (nonlinear optical rotational anisotropy, nonlinear optical microscopy and time-resolved optical reflectivity) to search for novel electronic phases in correlated electron materials. Using these techniques, we completed five major scientific projects. 1) We discovered previously unresolved oxygen sub-lattice distortions in layered perovskite iridates, which explain the anomalous magneto-elastic coupling and basal plane ferromagnetism observed in Sr₂IrO₄ and Sr₃Ir₂O₇ respectively. 2) We discovered a previously hidden odd-parity magnetic order in the pseudogap region of hole-doped Sr₂IrO₄, which is consistent with the long-sought orbital loop-current phase that has been conjectured to underlie the pseudogap region of the cuprate high-T_c superconductors. 3) We discovered a similar odd-parity magnetic order in the pseudogap region of hole-doped YBa₂Cu₃O₇ that appears to terminate at a quantum critical point inside the superconducting dome. 4) We discovered an ultrafast photo-induced insulator-to-metal phase transition in Ca₂RuO₄ that, unlike the phase transition in thermal equilibrium, is not accompanied by any structural distortion. 5) We revealed the weak Mott insulating character of Sr₃Ir₂O₇ and discovered the emergence of an unconventional density wave instability upon electron-doping that is reminiscent of the charge ordering recently reported in under-doped cuprates.

Enter List of papers submitted or published that acknowledge ARO support from the start of the project to the date of this printing. List the papers, including journal references, in the following categories:

(a) Papers published in peer-reviewed journals (N/A for none)

Received Paper

08/06/2014 1.00 Darius H. Torchinsky, Hao Chu, Tongfei Qi, Gang Cao, David Hsieh. A low temperature nonlinear optical rotational anisotropy spectrometer for the determination of crystallographic and electronic symmetries, *Review of Scientific Instruments*, (05 2014): 83102. doi:

08/16/2015 3.00 D.H. Torchinsky, H. Chu, L. Zhao, N.B. Perkins, Y. Sizuk, T. Qi, G. Cao, D. Hsieh. Structural Distortion-Induced Magnetoelastic Locking in Sr₂IrO₄ Revealed through Nonlinear Optical Harmonic Generation, *PHYSICAL REVIEW LETTERS*, (03 2015): 96404. doi:

TOTAL: **2**

Number of Papers published in peer-reviewed journals:

(b) Papers published in non-peer-reviewed journals (N/A for none)

Received Paper

TOTAL:

Number of Papers published in non peer-reviewed journals:

(c) Presentations

Revealing hidden orders in correlated electron systems with nonlinear optics. Conference on Lasers and Electro-Optics (CLEO), San Jose, (June 5-10, 2016).

Revealing hidden orders in correlated electron systems using nonlinear optics. Annual Conference of the Institute for Complex Adaptive Matter (ICAM), Kent State University, (May 16-18, 2016).

Hidden orders in perovskite iridates. Gordon Research Conference: Ultrafast Phenomena in Cooperative Systems, Lucca, Italy (February 14-19, 2016).

Hidden order in a perovskite iridate revealed by nonlinear optics. Topological Phases in Condensed Matter and Cold Atomic Systems, Hong Kong University of Science and Technology, (December 11-19, 2015).

Topological band and correlated insulators. Spin-Orbit Coupling and Relativistic Quantum Materials Summer School, University of British Columbia, (October 22-25, 2015).

Hidden order in a perovskite iridate revealed by nonlinear optics. New Phases and Emergent Phenomena in Correlated Materials with Strong Spin-Orbit Coupling, Kavli Institute for Theoretical Physics, (September 15, 2015).

Number of Presentations: 6.00

Non Peer-Reviewed Conference Proceeding publications (other than abstracts):

Received Paper

06/11/2016 7.00 . Revealing Hidden Orders in Correlated Electron Systems with Nonlinear Optics, CLEO: QELS_Fundamental Science. 06-JUN-16, San Jose, California. : ,

TOTAL: **1**

Number of Non Peer-Reviewed Conference Proceeding publications (other than abstracts):

Peer-Reviewed Conference Proceeding publications (other than abstracts):

Received Paper

TOTAL:

Number of Peer-Reviewed Conference Proceeding publications (other than abstracts):

(d) Manuscripts

Received Paper

06/11/2016 6.00 L. Zhao, D. H. Torchinsky, H. Chu, V. Ivanov, R. Lifshitz, R. Flint, T. Qi, G. Cao, D. Hsieh. Evidence of an odd-parity hidden order in a spin-orbit coupled correlated iridate, *Nature Physics* (08 2015)

08/06/2014 2.00 Liuyan Zhao, Hao Chu, Natalia B. Perkins, Yuriy Sizuk, Tongfei Qi, Darius H. Torchinsky, Gang Cao, David Hsieh. A structural distortion induced magneto-elastic locking in Sr₂IrO₄ revealed through nonlinear optical harmonic generation, *Physical Review Letters* (submitted) (07 2014)

08/16/2015 5.00 H. Chu, D. H. Torchinsky, L. Zhao, T. Deshpande, N. B. Perkins, P. Rall, J. W. Han, J. S. Lee, J. Terzic, G. Cao, D. Hsieh. Ultrafast photo-induced electronic phase transition in a perovskite ruthenate, *Physical Review Letters* (submitted) (07 2015)

TOTAL: **3**

Number of Manuscripts:

Books

Received Book

TOTAL:

Received Book Chapter

08/16/2015 4.00 D. H. Torchinsky, D. Hsieh. Rotational Anisotropy Nonlinear Harmonic Generation, Invited book chapter on "Magnetic characterization techniques for nanomaterials" : Springer, (12 2015)

TOTAL: **1**

Patents Submitted

Rotating Scattering Plane Based Nonlinear Optical Spectrometer to Study the Crystallographic and Electronic Symmetries of Crystals

Patents Awarded

Awards

Packard Fellowship in Science and Engineering (2015 - 2020)

Graduate Students

<u>NAME</u>	<u>PERCENT SUPPORTED</u>	Discipline
Hao Chu	0.69	
Tejas Deshpande	0.50	
FTE Equivalent:	1.19	
Total Number:	2	

Names of Post Doctorates

<u>NAME</u>	<u>PERCENT SUPPORTED</u>
Liuyan Zhao	0.32
Darius Torchinsky	1.00
FTE Equivalent:	1.32
Total Number:	2

Names of Faculty Supported

<u>NAME</u>	<u>PERCENT SUPPORTED</u>	National Academy Member
David Hsieh	0.01	
FTE Equivalent:	0.01	
Total Number:	1	

Names of Under Graduate students supported

<u>NAME</u>	<u>PERCENT SUPPORTED</u>
FTE Equivalent:	
Total Number:	

Student Metrics

This section only applies to graduating undergraduates supported by this agreement in this reporting period

The number of undergraduates funded by this agreement who graduated during this period: 0.00

The number of undergraduates funded by this agreement who graduated during this period with a degree in science, mathematics, engineering, or technology fields:..... 0.00

The number of undergraduates funded by your agreement who graduated during this period and will continue to pursue a graduate or Ph.D. degree in science, mathematics, engineering, or technology fields:..... 0.00

Number of graduating undergraduates who achieved a 3.5 GPA to 4.0 (4.0 max scale):..... 0.00

Number of graduating undergraduates funded by a DoD funded Center of Excellence grant for Education, Research and Engineering:..... 0.00

The number of undergraduates funded by your agreement who graduated during this period and intend to work for the Department of Defense 0.00

The number of undergraduates funded by your agreement who graduated during this period and will receive scholarships or fellowships for further studies in science, mathematics, engineering or technology fields:..... 0.00

Names of Personnel receiving masters degrees

NAME

Total Number:

Names of personnel receiving PhDs

NAME

Total Number:

Names of other research staff

NAME

PERCENT_SUPPORTED

FTE Equivalent:

Total Number:

Sub Contractors (DD882)

Inventions (DD882)

Scientific Progress

See Attachment

Technology Transfer

TABLE OF CONTENTS:

SECTION	PAGE NUMBER
1. Subtle structural distortions in the single and bilayer iridates	1
2. Discovery of a parity-odd hidden order in $\text{Sr}_2\text{Ir}_{1-x}\text{Rh}_x\text{O}_4$	2
3. Discovery of broken global inversion symmetry in $\text{YBa}_2\text{Cu}_3\text{O}_{6+x}$	4
4. Ultrafast photo-induced electronic phase transition in Ca_2RuO_4	6
5. Discovery of an unconventional density wave order in $(\text{Sr}_{1-x}\text{La}_x)_3\text{Ir}_2\text{O}_7$	8
Bibliography	10

Summary of the most important results

1. Subtle structural distortions in the single and bilayer iridates

The overarching motivation of this study was to resolve two outstanding questions in Sr_2IrO_4 . First, high resolution neutron diffraction studies in 2013 reported weak structural Bragg peaks that violated the long accepted tetragonal $4/mmm$ crystal point group symmetry of Sr_2IrO_4 ^{1,2}. Although several crystal structures with reduced symmetry were proposed, a unique structure was not able to be determined. Second, resonant x-ray diffraction studies reported a perfect locking of the magnetic moment canting angle and oxygen octahedral rotation angle below the Neel temperature³. However this could only be reconciled with the well-known Jackeli-Khaliullin model of the iridates⁴ by finely tuning the spin-orbit coupling and tetragonal crystal field splitting energies to values that lay outside those experimentally determined for Sr_2IrO_4 .

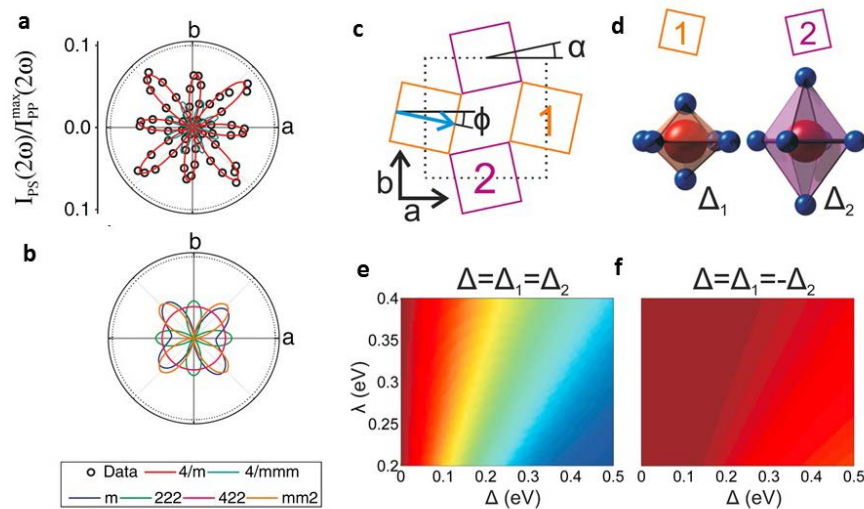


Fig. 1 **a**, Second harmonic generation rotational anisotropy (SHG-RA) pattern of Sr_2IrO_4 (001) taken under PS polarization geometry at $T = 295$ K. Red and cyan lines are best fits to bulk electric quadrupole induced SHG-RA calculated using centrosymmetric $4/m$ and $4/mmm$ point groups respectively. **b**, shows best fits to bulk electric dipole induced SHG calculated using the three proposed non-centrosymmetric point groups $mm2$, 222 and 422 as well as the monoclinic point group m for comparison. Responses that are absent in the plots are symmetry forbidden. **c**, Illustration of an IrO_2 plane in Sr_2IrO_4 . The oxygen octahedra rotate about the c -axis by $\pm\alpha$ creating a two sub-lattice structure. The magnetic moments couple to the lattice and exhibit canting angles $\pm\phi$. **d**, An unequal tetragonal distortion (Δ_1 and Δ_2) on the two sub-lattices as required by the $4/m$ point group. **e**, The ratio ϕ/α as a function of both spin-orbit coupling λ and tetragonal crystal field splitting Δ calculated for the case of uniform and **f**, staggered ($\Delta_1 = -\Delta_2$) tetragonal distortion.

To resolve the crystal structure of Sr_2IrO_4 , we directly measured the structure of its optical second harmonic susceptibility tensor using a novel low temperature rotational anisotropy technique developed with support from an ARO DURIP Award (W911NF-13-1-0293)⁵. By fitting the data to calculations using the different crystallographic point groups proposed by neutron scattering studies (Fig. 1a,b), we found that Sr_2IrO_4 crystallizes in the lower $4/m$ point group due a staggered tetragonal distortion of the oxygen octahedral (Fig. 1c,d). This contrasts with the case of a $4/mmm$ point group, which is constrained to having a uniform tetragonal distortion. This staggering gives rise to an alternating crystal field splitting energy (Δ_1 and Δ_2) from one Ir site to another. By studying an effective super-exchange Hamiltonian that accounts for this alternation, we found that perfect locking ($\alpha=\varphi$) between the oxygen octahedral rotation angle and magnetic moment canting angle is preserved over a large range of spin-orbit coupling energies and crystal field splitting energies (Fig. 1e,f), which resolves the previous discrepancy between experiments and theory.

The $4/m$ symmetry uncovered by our second harmonic generation measurements was subsequently corroborated by high resolution neutron diffraction experiments⁶, highlighting the power of our technique to perform detailed structural symmetry refinement. Similar second harmonic generation measurements were more recently performed on $\text{Sr}_3\text{Ir}_2\text{O}_7$ ⁷, which also revealed a subtle monoclinic distortion of the oxygen sub-lattice that explains the anomalous in-plane ferromagnetic moment observed in magnetic susceptibility measurements.

The Sr_2IrO_4 work was performed in collaboration with Prof. Natalia Perkins (University of Minnesota) and Prof. Gang Cao (University of Colorado at Boulder) and was published in Physical Review Letters. The $\text{Sr}_3\text{Ir}_2\text{O}_7$ work was performed in collaboration with Prof. Stephen Wilson (University of California at Santa Barbara) and was published in Physical Review B.

2. Discovery of a parity-odd hidden order in $\text{Sr}_2\text{Ir}_{1-x}\text{Rh}_x\text{O}_4$

The perovskite iridate Sr_2IrO_4 is a promising host for exotic phases that emerge from an interplay of strong spin-orbit coupling and strong electron-electron correlations. The resemblance of its crystallographic, magnetic and electronic structures to La_2CuO_4 , as well as the emergence upon doping of a pseudogap region^{8–10} and a low temperature d -wave gap^{11,12}, has particularly strengthened analogies to cuprate high- T_c superconductors. However, unlike the cuprate phase diagram that features a plethora of broken symmetry phases in a pseudogap region that include charge density wave, stripe, nematic and possibly intra-unit cell loop-current orders, no broken symmetry phases proximate to the parent antiferromagnetic Mott insulating phase in Sr_2IrO_4 have been observed to date, making the comparison of iridate to cuprate phenomenology incomplete. In this work, we reveal an unusual hidden order in Sr_2IrO_4 using the novel optical second harmonic generation (SHG) rotational anisotropy and microscopy techniques that we developed⁵ and demonstrated¹³ during years 1 – 2 of this award.

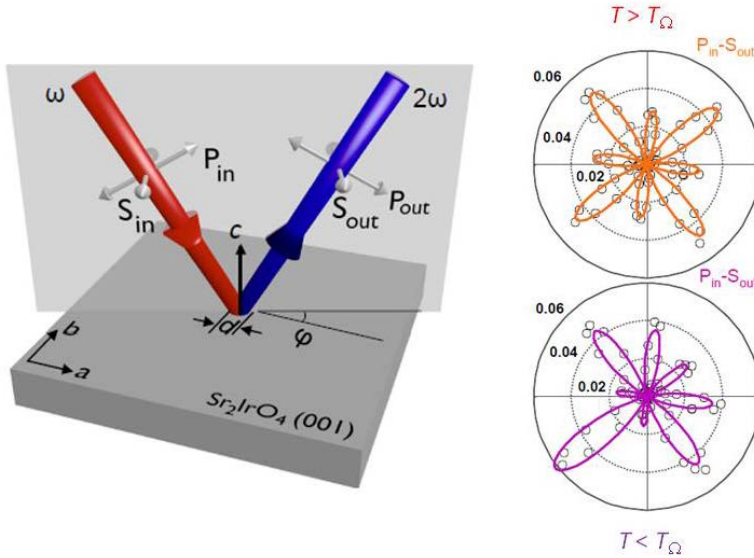


Fig. 2. (Left) Schematic layout of the RA-SHG experiment. The scattering plane defined by the incident fundamental beam (red) and reflected SHG beam (blue) is rotated about the crystallographic c -axis. (Right) The RA-SHG patterns acquired from the (001) cleaved surface of Sr_2IrO_4 above and below the hidden ordering temperature T_Ω . The orange curve is a fit to a non-magnetic tetragonal point group while the purple curve includes a contribution from a magnetic inversion broken point group.

The symmetry properties of this hidden order are very unusual. It preserves lattice translational symmetry and its order parameter is non-dipolar in nature, which has precluded its detection by conventional diffraction and dc susceptibility probes. However, our nonlinear optical probe shows that it is magnetic in origin and breaks both the 4-fold rotational symmetry and inversion symmetry of the underlying tetragonal lattice (Fig. 2). The onset temperature T_Ω of this hidden order is close to the Neel transition temperature T_N in the undoped Sr_2IrO_4 compound, but they bifurcate upon hole doping (Fig. 3a-c) to reveal an extensive region of the phase diagram with purely hidden order (Fig. 3d).

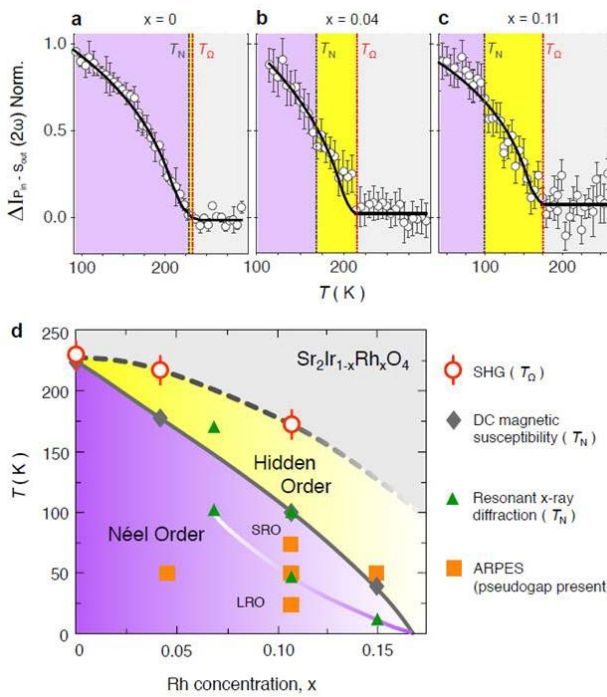


Fig. 3. **a**, The change in SHG intensity from $\text{Sr}_2\text{Ir}_{1-x}\text{Rh}_x\text{O}_4$ at $x = 0$, **b**, $x = 0.04$ and **c**, $x = 0.11$ measured relative to their room temperature values as a function of temperature. Lines are guides to the eye. The dashed red lines mark the transition temperature T_Ω of the hidden order phase deduced from our SHG data and the dashed black lines mark the Neel temperature T_N determined from dc magnetic susceptibility measurements. **d**, Temperature versus doping phase diagram of $\text{Sr}_2\text{Ir}_{1-x}\text{Rh}_x\text{O}_4$ showing the boundaries of the hidden order and the long-range (LRO) and short-range (SRO) Neel ordered regions. Points where a pseudogap has been measured are also marked.

The symmetry properties of this hidden order are consistent with a so-called “magneto-electric loop-current” phase, which has long been conjectured to exist in and possibly be responsible for the pseudogap region of the cuprates although experimentally the issue remains unsettled. The presence of a loop-current phase in the pseudogap region of Sr_2IrO_4 would provide a testbed for these ideas and thus further experiments are already in progress to understand the microscopic origin of this hidden order in Sr_2IrO_4 and its relationship with the pseudogap.

This work was performed in collaboration with Prof. Rebecca Flint (Ohio State University), Prof. Ron Lifshitz (Tel Aviv University) and Prof. Gang Cao (University of Kentucky) and is published in *Nature Physics*.

3. Discovery of broken global inversion symmetry in $\text{YBa}_2\text{Cu}_3\text{O}_{6+x}$

Understanding the nature of the pseudogap region is widely considered to be essential for revealing the mechanism of high- T_c superconductivity in the copper oxides. Within the last few years, there has been an infusion of experimental evidence that the pseudogap is a bona fide thermodynamic phase of matter with distinct broken symmetries¹⁴. However, exactly what set of symmetries are broken, and in turn what microscopic ordering phenomenon is occurring, remain unsettled questions. Moreover, the fate of this underlying order upon transitioning from the pseudogap region into the superconducting dome is unknown.

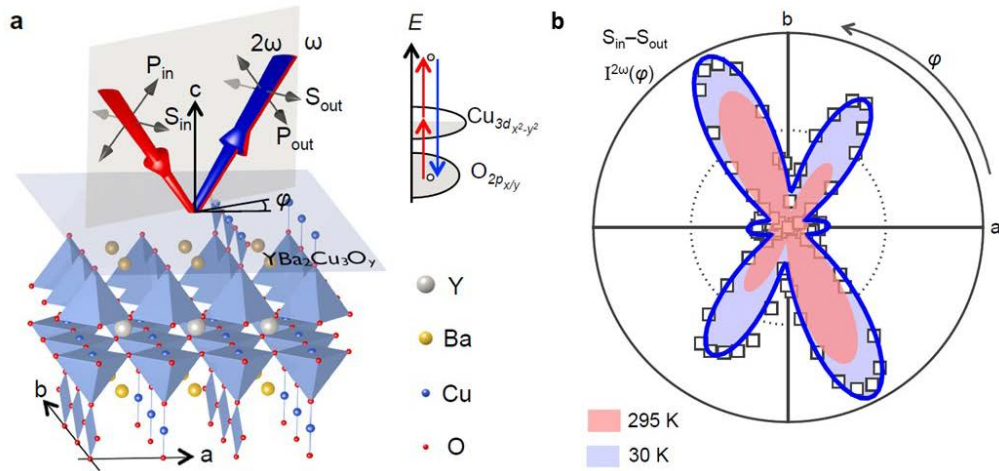


Fig. 4 **a**, The intensity of light reflected at the fundamental (I^ω) and second harmonic ($I^{2\omega}$) frequencies of an obliquely incident beam is measured as a function of the angle (φ) between the scattering plane and the a - c plane of $\text{YBa}_2\text{Cu}_3\text{O}_y$. The incident photon energy (1.5 eV) is resonant with the O $2p$ to Cu $3d$ charge transfer transition (inset). **b**, Polar plot of $I^{2\omega}(\varphi)$ measured below (squares; blue area) and above (red area; consistent with $2/m$ symmetry) the pseudogap temperature ($T^* \sim 110$ K) of $\text{YBa}_2\text{Cu}_3\text{O}_{6.92}$ with both the incident and reflected beams polarized perpendicular to the scattering plane ($S_{\text{in}}-S_{\text{out}}$ geometry).

The reason for this incomplete understanding is that the experimental techniques that have so far managed to successfully detect broken symmetries across the pseudogap phase boundary (i.e. polarized neutron diffraction¹⁵, THz conductivity¹⁶, transport anisotropy¹⁷ and resonant ultrasound spectroscopy¹⁸) have several limitations: i) they are sensitive only to specific symmetry operations, ii) they are volume integrated and thus potentially blind to certain broken symmetries due to domain averaging, iii) the symmetry of the material can only clearly be measured by THz conductivity inside the pseudogap region, which precludes identification of changes in symmetry across the pseudogap phase boundary, iv) broken symmetry features in resistivity/Nernst anisotropy and polarized neutron diffraction data become obscured by the effects of superconductivity inside the dome, and v) resonant ultrasound spectroscopy is only sensitive to lattice distortions and is so far unable to resolve specific broken symmetries.

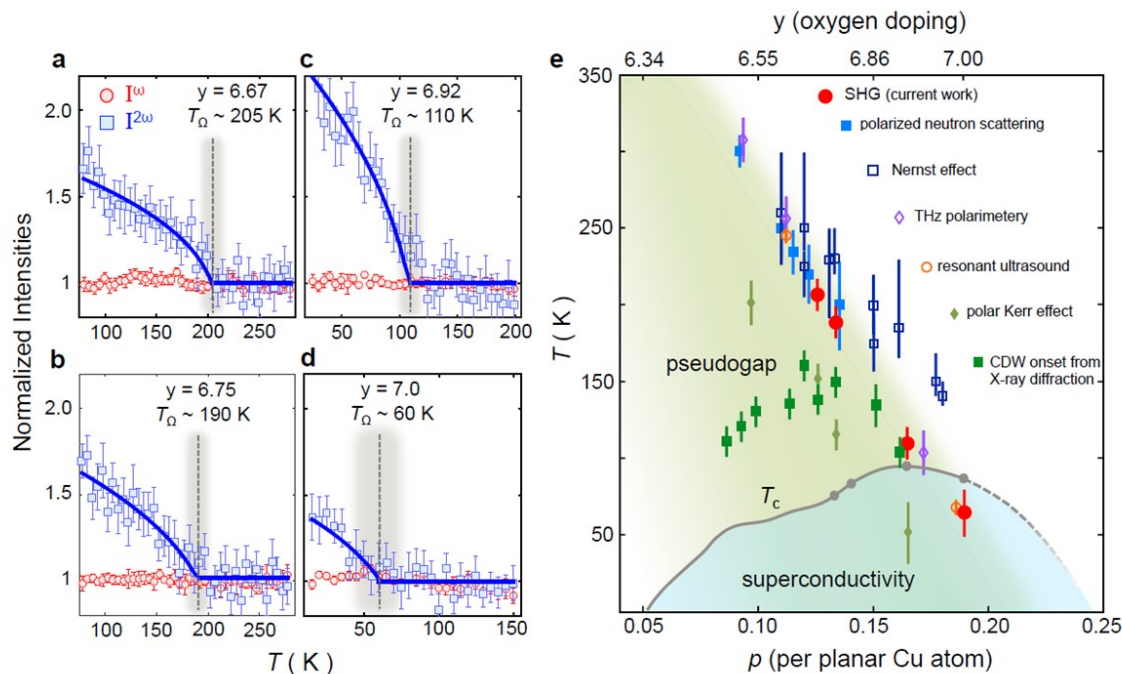


Fig. 5 Temperature dependence of I^ω and $I^{2\omega}$ of $\text{YBa}_2\text{Cu}_3\text{O}_y$ with **a**, $y = 6.67$, **b**, 6.75, **c**, 6.92 and **d**, 7.0 normalized to their room temperature values. Data were taken in $S_{\text{in}}\text{--}S_{\text{out}}$ geometry at a fixed φ . The upturn in $I^{2\omega}$ at T_Ω (gray line) and lack thereof in I^ω is a signature of global inversion symmetry breaking. **e**, Temperature versus doping phase diagram of $\text{YBa}_2\text{Cu}_3\text{O}_y$. The values of T_Ω (red circles) coincide with the onset of the pseudogap as defined by the other techniques listed.

As discussed in the previous two sections, in this ARO program we developed a new and powerful technique to measure the complete crystallographic and electronic symmetry group of a material based on studying the rotational anisotropy of its nonlinear optical response⁵. Over the course of this program, we used this technique to uncover previously hidden structural distortions in Sr_2IrO_4 ¹³ and $\text{Sr}_3\text{Ir}_2\text{O}_7$ ⁷ as well as a novel multipolar electronic order in the

pseudogap region of hole-doped Sr_2IrO_4 ¹⁹. By applying this technique to a prototypical cuprate high- T_c superconductor $\text{YBa}_2\text{Cu}_3\text{O}_y$ (Fig. 4a), we successfully resolved the full symmetry group of the pseudogap, strange metal and superconducting regions of the temperature versus hole-doping phase diagram for the first time in any cuprate.

Our work reveals the following new information: 1) The strange metal phase of $\text{YBa}_2\text{Cu}_3\text{O}_y$ has the monoclinic $2/m$ point group symmetry as opposed to the previously believed orthorhombic mmm point group symmetry (Fig. 4b). 2) Across the strange metal to pseudogap boundary, spatial inversion, two-fold rotation and time-reversal symmetries are broken (Fig. 5a-d), yielding either a $2'/m$ or $m1'$ magnetic point group. Although time-reversal symmetry breaking was also previously reported by polarized neutron diffraction, spatial inversion and two-fold rotational symmetry breaking have never been previously observed. 3) This symmetry breaking phase transition occurs even inside the superconducting dome, pointing towards a quantum phase transition inside the dome on the slightly over-doped side of the phase diagram (Fig. 5e). 4) The order parameter of this pseudogap phase does not compete with either the superconducting or charge density wave order parameters. Taken together, these results drastically narrow down the list of possible candidates for the microscopic phase underlying the pseudogap region, favoring only those with an odd-parity magnetic order parameter that do not arise from a competing Fermi surface instability.

This work was performed in collaboration with Prof. Ruixing Liang, Doug Bonn and Walter Hardy (University of British Columbia) and Prof. Peter Armitage (The Johns Hopkins University) and is being submitted to *Nature*.

4. Ultrafast photo-induced electronic phase transition in Ca_2RuO_4

Over the past decade there has been a great deal of interest in searching for ultrafast optically induced electronic phase transitions in solids. Impulsive optical excitation provides an opportunity to access fundamentally new driven electronic phases that would otherwise be impossible to realize in thermal equilibrium. Transition metal oxides offer a promising platform for realizing such phenomena because many different phases can often be stabilized through only a slight rebalancing of competing microscopic interactions, making them highly sensitive to external stimuli such as light. To date, examples of this effect have been discovered in several $3d$ transition metal oxides, with the photo-induced structural and insulator-to-metal transitions in VO_2 being perhaps the most well-known.

Heavier $4d$ and $5d$ transition metal oxides have recently drawn a lot of attention because there is often a greater level of competition between microscopic energy scales compared to $3d$ transition metal oxides, which can produce exotic electronic phases in thermal equilibrium. The perovskite ruthenate Ca_2RuO_4 is a notable example where competing kinetic, Coulomb and crystal field

energy scales put the system at a phase boundary between an electrically isotropic metal and a structurally distorted orbital polarized Mott insulator. However, despite widespread efforts to search for new equilibrium phases in heavy (non-3d) transition metal oxide systems, their potential for hosting interesting non-equilibrium driven phases is completely unexplored.

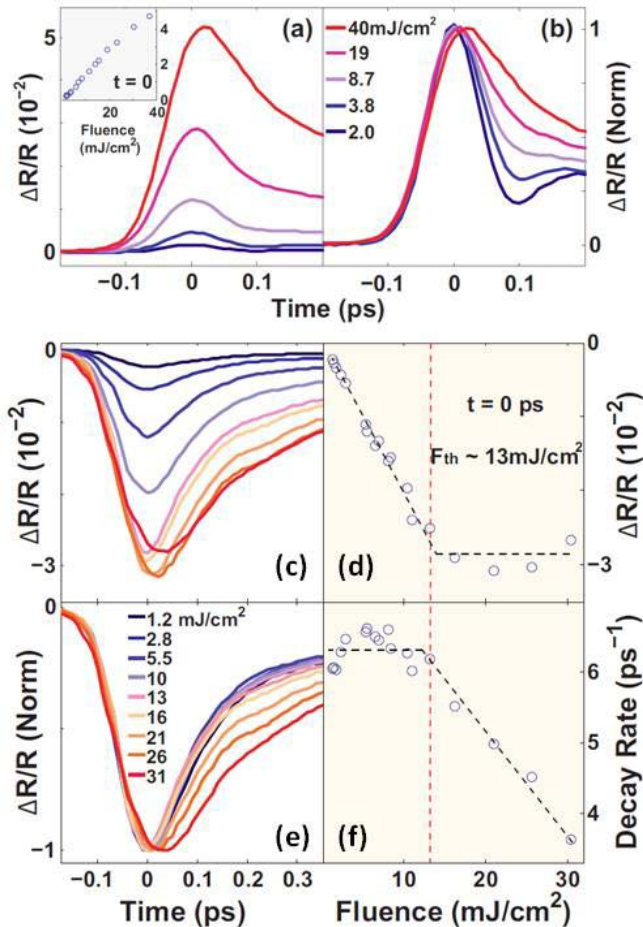


Fig. 6 Pump fluence dependence of the **a**, unnormalized and **b**, normalized $\Delta R/R$ traces of Ca_2RuO_4 at $T > T_{\text{IMT}}$. Inset shows the fluence dependence of the value of $\Delta R/R$ at $t = 0$. **c**, Pump fluence dependence of the un-normalized $\Delta R/R$ traces at $T < T_{\text{IMT}}$ and **d**, their values at $t = 0$. **e**, Pump fluence dependence of the normalized $\Delta R/R$ traces at $T < T_{\text{IMT}}$ and **f**, their initial decay rates.

distortion. This type of optically driven dynamic decoupling between electronic and lattice degrees of freedom is very similar to that recently discovered in VO_2 under weak optical excitation²⁰ and, more generally, shows that heavier transition metal oxides can provide a platform for realizing driven electronic phases that are not accessible in thermal equilibrium. Time-resolved reflectivity experiments using probe photon energies smaller than the Mott gap

In this work we present the first evidence of an optically driven electronic phase transition in a 4d transition metal oxide Ca_2RuO_4 using ultrafast time-resolved pump-probe optical reflectivity. Figures 6a and b show that above the insulator-to-metal transition temperature (T_{IMT}) of Ca_2RuO_4 , the differential reflectivity transients ($\Delta R/R$) exhibit a peak value that increases linearly with pump fluence and an initial decay rate that decreases monotonically with fluence. Below T_{IMT} and at low fluences, the negative peak value of $\Delta R/R$ continues to scale linearly with fluence (Fig. 6c,d) while the decay dynamics of the reflectivity transients are fluence independent (Fig. 6e,f). Surprisingly however, we discovered a critical fluence ($\sim 13 \text{ mJ/cm}^2$) above which the peak value abruptly saturates and the decay dynamics acquire a fluence dependence similar to the $T > T_{\text{IMT}}$ case. These features are consistent with an electronic phase transition taking place above the critical fluence and highly suggest that it is an insulator-to-metal transition. Moreover, unlike all previous studies of the insulator-to-metal transition in Ca_2RuO_4 that were conducted in thermal equilibrium, our observed non-equilibrium transition is not accompanied by a structural

are currently underway to examine whether the photoinduced transition is indeed between an insulating and metallic phase.

This work was performed in collaboration with Prof. Jong Seok Lee (Gwangju Institute of Science and Technology) and Prof. Gang Cao (University of Kentucky). The manuscript is currently under review at Physical Review Letters.

5. Discovery of an unconventional density wave order in $(\text{Sr}_{1-x}\text{La}_x)_3\text{Ir}_2\text{O}_7$

Over the past several years there has been growing interest in insulating iridium oxide based materials because they are believed to realize a rare type of Mott insulator that is stabilized by the cooperative effects of electron-electron correlations and spin-orbit coupling²¹. There is particular focus on the layered perovskite family of iridates ($\text{Sr}_{n+1}\text{Ir}_n\text{O}_{3n+1}$) because of their structural and possible electronic resemblance to the parent compounds of the cuprate high- T_c superconductors.

The iridate Mott insulators are unfortunately very difficult to chemically dope, which has made it challenging to achieve a detailed understanding of their temperature versus doping phase diagrams. Recently however, several groups have succeeded in doping both the single ($n=1$) and bilayer ($n=2$) members away from the Mott insulating parent state and into true metallic regimes, which presents a unique opportunity to carefully examine their parallels to cuprates. This has already led to several recent high profile discoveries in doped Sr_2IrO_4 including a pseudogap phase⁸⁻¹⁰, a multipolar ordered phase¹⁹ and a possible *d*-wave superconducting phase^{11,12}, which have strengthened the analogy between iridates and cuprates. Surprisingly however, no electronic instabilities have been reported in doped $\text{Sr}_3\text{Ir}_2\text{O}_7$ by any experimental technique so far, challenging the validity of any comparison to the bilayer cuprates.

This project addresses two questions: 1) Is the Mott state in $\text{Sr}_3\text{Ir}_2\text{O}_7$ in fact comparable to the parent state of cuprates and 2) Is the Fermi surface that emerges in doped $\text{Sr}_3\text{Ir}_2\text{O}_7$ truly stable against any type of electronic order? Our findings are as follows: 1) The Mott state in $\text{Sr}_3\text{Ir}_2\text{O}_7$ is only marginally stable and does not belong to the same strongly correlated Mott insulator regime that describes the cuprate parent compounds. We show this by uncovering the concurrence of gap opening with antiferromagnetic ordering in $\text{Sr}_3\text{Ir}_2\text{O}_7$ using an ultrafast time-resolved pump-probe optical reflectivity setup, which was developed with support from an ARO DURIP Award (W911NF-13-1-0293). This connection was not possible to establish using conventional techniques such as STM²², ARPES^{23,24} or optical conductivity²⁵ due to the challenge of resolving small energy scales at high temperatures. 2) Doped $\text{Sr}_3\text{Ir}_2\text{O}_7$ actually does undergo an electronic phase transition into an unusual density wave like state at relatively high temperatures of order 200 K. This electronic ordering was only possible to uncover by temporally resolving coherent oscillations of its order parameter using time-resolved optical reflectivity and was found to exist over an extended region of the temperature versus doping phase diagram (Fig. 7).

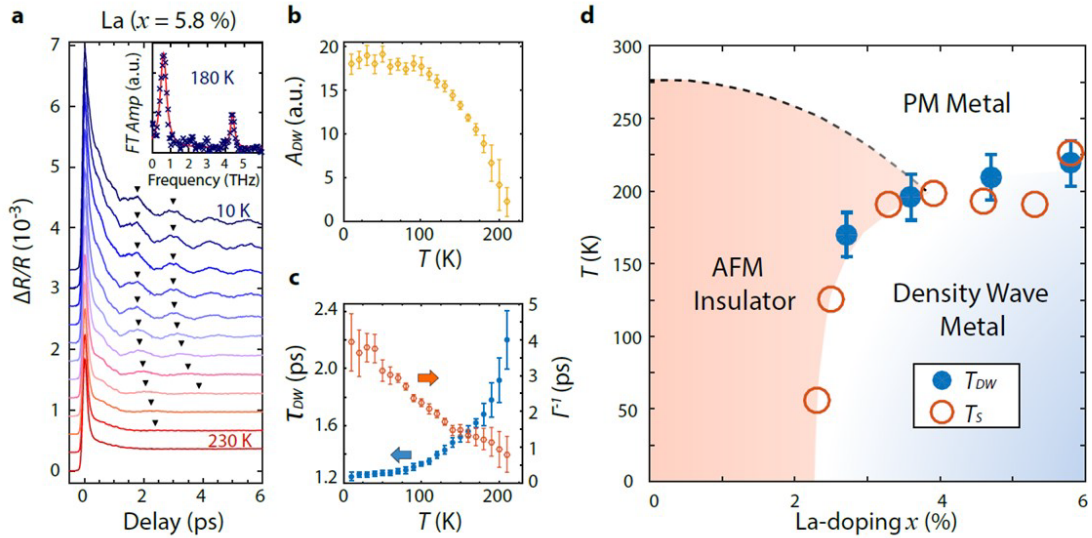


Fig. 7 **a**, Pump-induced change in optical reflectivity of $(\text{Sr}_{1-x}\text{La}_x)_3\text{Ir}_2\text{O}_7$ ($x = 0.058$) plotted for a series of temperatures separated by 20 K showing temporal modulations due to coherent density wave oscillations. Two of the modulation peaks are marked with triangles to guide the eye. The Fourier transform of the background subtracted reflectivity transient measured at 180 K is shown in the inset. **b**, Temperature dependence of the oscillation amplitude A_{DW} and **c**, period (T_{DW}) and damping time (Γ^{-1}). **d**, Temperature versus doping (x) phase diagram. The paramagnetic (PM) to antiferromagnetic (AFM) phase boundary and the line of structural transitions (T_s) are based on data from Ref. [22] whereas the line of density wave phase transitions (T_{DW}) is based on the current work.

Our results settle the nature of the insulating state in $\text{Sr}_3\text{Ir}_2\text{O}_7$ and provide a starting point for understanding the contrasting phenomenology of the bilayer iridates and cuprates. Our work also reveals an unusual density wave like order in doped $\text{Sr}_3\text{Ir}_2\text{O}_7$, which is reminiscent of the charge density wave order recently observed in cuprates in the sense that it eludes most conventional probes due possibly to a temporally fluctuating or spatially short-ranged nature. Regardless of microscopic origin, this work dispels previous notions that the Fermi surface of doped $\text{Sr}_3\text{Ir}_2\text{O}_7$ is electronically inert and is anticipated to ignite efforts to search for other competing phases in $\text{Sr}_3\text{Ir}_2\text{O}_7$ in parallel with existing efforts on Sr_2IrO_4 . We believe that this work will also stimulate theoretical attention towards models in the strongly spin-orbit coupled weak Mott regime, which have been less studied than their strong Mott counterparts, and drive high quality materials synthesis efforts both in single crystal and thin film form like what we are currently witnessing for Sr_2IrO_4 .

This work was performed in collaboration with Prof. Stephen Wilson (University of California at Santa Barbara) and is currently under review at *Nature Materials*.

Bibliography

1. Ye, F. *et al.* Magnetic and crystal structures of Sr_2IrO_4 : A neutron diffraction study. *Phys. Rev. B* **87**, 140406 (2013).
2. Dhital, C. *et al.* Neutron scattering study of correlated phase behavior in Sr_2IrO_4 . *Phys. Rev. B* **87**, 144405 (2013).
3. Boseggia, S. *et al.* Locking of iridium magnetic moments to the correlated rotation of oxygen octahedra in Sr_2IrO_4 revealed by x-ray resonant scattering. *J. Phys. Condens. Matter* **25**, 422202 (2013).
4. Jackeli, G. & Khaliullin, G. Mott Insulators in the Strong Spin-Orbit Coupling Limit: From Heisenberg to a Quantum Compass and Kitaev Models. *Phys. Rev. Lett.* **102**, 17205 (2009).
5. Torchinsky, D. H., Chu, H., Qi, T., Cao, G. & Hsieh, D. A low temperature nonlinear optical rotational anisotropy spectrometer for the determination of crystallographic and electronic symmetries. *Rev. Sci. Instrum.* **85**, 83102 (2014).
6. Ye, F. *et al.* Structure symmetry determination and magnetic evolution in $\text{Sr}_2\text{Ir}_{1-x}\text{Rh}_x\text{O}_4$. *Phys. Rev. B* **92**, 201112 (2015).
7. Hogan, T. *et al.* Structural investigation of the bilayer iridate $\text{Sr}_3\text{Ir}_2\text{O}_7$. *Phys. Rev. B* **93**, 134110 (2016).
8. Kim, Y. K. *et al.* Fermi arcs in a doped pseudospin-1/2 Heisenberg antiferromagnet. *Science* **345**, 187–190 (2014).
9. de la Torre, A. *et al.* Collapse of the Mott Gap and Emergence of a Nodal Liquid in Lightly Doped Sr_2IrO_4 . *Phys. Rev. Lett.* **115**, 176402 (2015).
10. Cao, Y. *et al.* Hallmarks of the Mott-metal crossover in the hole-doped pseudospin-1/2 Mott insulator Sr_2IrO_4 . *Nat. Commun.* **7**, 11367 (2016).
11. Kim, Y. K., Sung, N. H., Denlinger, J. D. & Kim, B. J. Observation of a d-wave gap in electron-doped Sr_2IrO_4 . *Nat. Phys.* **12**, 37–41 (2016).
12. Yan, Y. J. *et al.* Electron-Doped Sr_2IrO_4 : An Analogue of Hole-Doped Cuprate Superconductors Demonstrated by Scanning Tunneling Microscopy. *Phys. Rev. X* **5**, 41018 (2015).
13. Torchinsky, D. H. *et al.* Structural Distortion-Induced Magnetoelastic Locking in Sr_2IrO_4 Revealed through Nonlinear Optical Harmonic Generation. *Phys. Rev. Lett.* **114**, 96404 (2015).
14. Keimer, B., Kivelson, S. A., Norman, M. R., Uchida, S. & Zaanen, J. From quantum matter to high-temperature superconductivity in copper oxides. *Nature* **518**, 179–186 (2015).
15. Fauqué, B. *et al.* Magnetic Order in the Pseudogap Phase of High-T_C Superconductors. *Phys. Rev. Lett.* **96**, 197001 (2006).
16. Lubashevsky, Y., Pan, L., Kirzhner, T., Koren, G. & Armitage, N. P. Optical Birefringence and Dichroism of Cuprate Superconductors in the THz Regime. *Phys. Rev. Lett.* **112**, 147001 (2014).
17. Daou, R. *et al.* Broken rotational symmetry in the pseudogap phase of a high-T_C superconductor. *Nature* **463**, 519–522 (2010).

18. Shekhter, A. *et al.* Bounding the pseudogap with a line of phase transitions in $\text{YBa}_2\text{Cu}_3\text{O}_{6+\delta}$. *Nature* **498**, 75–77 (2013).
19. Zhao, L. *et al.* Evidence of an odd-parity hidden order in a spin-orbit coupled correlated iridate. *Nat. Phys.* **12**, 32–36 (2016).
20. Morrison, V. R. *et al.* A photoinduced metal-like phase of monoclinic VO_2 revealed by ultrafast electron diffraction. *Science* **346**, 445–448 (2014).
21. Kim, B. J. *et al.* Novel $J_{\text{eff}}=1/2$ Mott State Induced by Relativistic Spin-Orbit Coupling in Sr_2IrO_4 . *Phys. Rev. Lett.* **101**, 76402 (2008).
22. Hogan, T. *et al.* First-Order Melting of a Weak Spin-Orbit Mott Insulator into a Correlated Metal. *Phys. Rev. Lett.* **114**, 257203 (2015).
23. de la Torre, A. *et al.* Coherent Quasiparticles with a Small Fermi Surface in Lightly Doped $\text{Sr}_3\text{Ir}_2\text{O}_7$. *Phys. Rev. Lett.* **113**, 256402 (2014).
24. He, J. *et al.* Spectroscopic evidence for negative electronic compressibility in a quasi-three-dimensional spin-orbit correlated metal. *Nat. Mater.* **14**, 577–582 (2015).
25. Park, H. J. *et al.* Phonon-assisted optical excitation in the narrow bandgap Mott insulator $\text{Sr}_3\text{Ir}_2\text{O}_7$. *Phys. Rev. B* **89**, 155115 (2014).